 CMES, vol.100, no.6, pp.477-506, 2014

Static, Free Vibration and Buckling Analysis of Functionally Graded Beam via B-spline Wavelet on the Interval and Timoshenko Beam Theory

Hao Zuo[1,2], Zhi-Bo Yang[1,2,3], Xue-Feng Chen[1,2], Yong Xie[4], Xing-Wu Zhang[1,2] and Yue Liu[5]

Abstract: The application of B-spline wavelet on the interval (BSWI) finite element method for static, free vibration and buckling analysis in functionally graded (FG) beam is presented in this paper. The functionally graded material (FGM) is a new type of heterogeneous composite material with material properties varying continuously throughout the thickness direction according to power law form in terms of volume fraction of material constituents. Different from polynomial interpolation used in traditional finite element method, the scaling functions of BSWI are employed to form the shape functions and construct wavelet-based elements. Timoshenko beam theory and Hamilton's principle are adopted to formulate the governing motion equations of FG beam. On account of the excellent approximation property of B-spline function for structure analysis, the proposed BSWI method could achieve a fast convergence and satisfying numerical results with fewer degrees of freedoms. In the end, different numerical examples are employed to demonstrate the validity and high accuracy of the formulated FGM BSWI element comparing with the exact solutions and other existing approaches in literatures. The numerical results also show that the proposed numerical algorithm is very suitable to investigate the static, free vibration and buckling analysis of FG beam.

Keywords: Functionally graded beam, wavelet finite element method, B-spline wavelet on the interval, Static analysis, Free vibration analysis, Buckling analysis.

[1] The State Key Laboratory for Manufacturing Systems Engineering, Xi'an, P.R. China.
[2] School of Mechanical Engineering, Xi'an Jiaotong University, Xi'an, P.R. China.
[3] Corresponding author. Tel: +86 18092795291; Fax: +86 29 82663689.
E-mail address: yangbo-5-7@163.com
[4] School of Aerospace, Xi'an Jiaotong University, Xi'an, P.R. China.
[5] Communication and Information Engineering College, Xi'an University of Science and Technology, Xi'an, P.R. China.

1 Introduction

The concept of functionally graded material (FGM) was initially proposed as advanced heat-shielding structural materials by Japanese scientists in 1987 [Koizumi (1993); Koizumi (1997)]. The FGM is a new type of heterogeneous composite material with material properties, such as Young's modulus and mass density, varying continuously throughout the thickness or length direction. Typically, FGM is composed of metallic and ceramic ingredients with the excellent property of metal for toughness, high thermal conductivity, machinability and good performance of ceramics for heat-shielding, high strength and corrosion resistant. Furthermore, the continuous changes in composition, microstructure and porosity lead to smooth changes in FGM which have many advantages over conventional composite materials where the de-lamination and cracks are most likely to generate at the interfaces due to the abrupt variation in mechanical properties between laminates. Such excellent performances make FG beam be widely used in structural fields such as aerospace industries, automotive applications, biomedical materials, optical components and fusion energy devices [Suresh et al. (1998)]. Therefore, the knowledge of static, dynamic and stability analysis of FG beam is very important for structural design, optimization and safety evaluation during their serviceable life.

Since FGM was presented in late l980s, many beam theories have been developed to investigate the static, free vibration and buckling of FG beam. The simplest classical beam theory (CBT), also known as Euler-Bernoulli beam theory, neglects the transverse shear deformation effect and gives satisfying results for slender FG beam only as presented by Sankar [Sankar (2001)], Aydogdu [Aydogdu (2008)], Alshorbagy et al. [Alshorbagy et al. (2011)]. The effect of transverse shear deformation becomes remarkable with the increasing thickness of FG beam, so the CBT would underestimate deflections and overestimate natural frequencies and buckling loads for moderately thick FG beam. To overcome this drawback, the first order shear deformation beam theory (FSDBT) known as Timoshenko beam theory has been developed for FG beam by considering the transverse shear deformation effect. Excellent works on the static and dynamic of FG beam have been carried out by Chakraborty et al. [Chakraborty et al. (2003)], Sina et al. [Sina et al. (2009)] on account of the high efficiency and simplicity of FSDBT. However, the FSDBT requires a shear correction factor which depends on various parameters such as geometric parameters, boundary conditions and loading conditions. For this reason, different higher order shear deformation beam theories (HSDBTs) have been proposed to avoid using shear correction factor. Their works mainly focused on the static and dynamic behavior of FG beam such as Aydogdu [Aydogdu and Taskin (2007)], Kadoli et al. [Kadoli et al. (2008)], Kapuria et al. [Kapuria et al. (2008)], Benatta et al. [Benatta et al. (2008)], Şimşek [Şimşek (2009); Şimşek and Ko-

catürk (2009); Şimşek (2010b)], Mahi et al. [Mahi et al. (2010)], Li [Li (2008); Li et al. (2010)], Wattanasakulpong et al. [Wattanasakulpong et al. (2011)], Thai and Vo [Thai and Vo (2012)]. Although HSDBTs could achieve accurate solutions without using shear correction factors, their governing equations are much more complicated than those of CBT and FSDBT.

The other main literatures concerning the problems of FG beam are briefly introduced as follows. Zhu and Sankar [Zhu and Sankar (2004)] proposed Fourier series-Galerkin method to analyze the stress of FG beam. Huang and Li [Huang and Li (2010)] proposed a novel and simple approach for free vibration of axially graded and non-uniform cross-section beams with various end supports. Atmane et al. [Atmane et al. (2011)] studied the free vibration behavior of FG beams with varying cross-section. Mazzei and Scott [Mazzei and Scott (2013)] investigated vibrations and static stability of tapered shafts. Rayleigh-Ritz method was employed for free vibration analysis of FG beam subjected to different boundary conditions by Pradhan and Chakraverty [Pradhan and Chakraverty (2013)]. Pradhan and Chakraverty [Pradhan and Chakraverty (2014)] studied vibration characteristic of FG beam subjected to three different sets of boundary conditions based on seven various deformation beam theories in Rayleigh-Ritz method. In their work, the authors summarized the influence of slenderness ratios, power-law variation of material properties, different material distributions and HSDBTs on the vibration characteristic of FG beam. Recently, Dong [Dong et al. (2014b); Dong et al. (2014a)] developed a simple 4-node and 3D 8-node locking-alleviated mixed finite element (CEQ4 and CEH8) for FG beam and plate structures. The developed element can accurately and effectively obtained not only the in-plane stress distribution and its variation in the thickness direction, but also the transverse shear stresses only using very few element.

Although many scholars concentrated their attentions on FG beam, studies on FG beam are relatively less and the literatures on the static and dynamic analysis of FG beam are still limited in numbers compared with FG plate and shell [Birman and Byrd (2007); Şimşek (2010a)]. And the literature on the buckling analysis of FG beam is rarely published and their research is mainly focus on thermal buckling [Wattanasakulpong et al. (2011)]. Furthermore, analytical solutions of FG beam are very difficult to find due to governing equations involve coefficients which depend upon spatial coordinates. Therefore, it is significant to develop a simple, validity and accurate numerical approach for the static, free vibration and buckling analysis of FG beam.

High performance numerical computation method is a powerful analysis tool for numerical simulation problems. Recently, some new numerical methods have been developed, such as meshless local Petrov-Galerkin (MLPG) method [Atluri and

Zhu (1998); Zhang et al. (2013)], local boundary integral equation (LBIE) method [Atluri et al. (1999); Atluri et al. (2000)], the discontinuous Galerkin method [Hartmann and Houston (2002)], the generalized differential quadrature (GDQ) method [Viola and Tornabene (2009)], the H-adaptive local radial basis function meshless method [Kosec and Šarler (2011)] and hybrid/mixed finite element [Dong and Atluri (2011)] etc. The wavelet finite element method (WFEM) is also a novel numerical method developed in recent years [Chen and Wu (1995); Xiang et al. (2010)]. Unlike the traditional finite element method, WFEM adopts scaling functions, instead of the polynomial interpolation used in traditional finite element method, to form the shape functions and construct wavelet-based elements. Compared with the interpolation wavelet function basis used now, B-spline wavelet on the interval (BSWI) basis has better characteristics in terms of compact support, smoothness and symmetry besides the multi-resolution analysis. Above all, BSWI has explicit expressions so that the coefficient integration and differentiation can be calculated conveniently. Therefore, BSWI is the best alternative choice in all the existing wavelets in approximation of numerical computing methods [Cohen (2003)]. Due to the excellent performance on numerical analysis, the WFEM adopting BSWI has been well developed by many researchers in structural analysis fields [Wu and Chen (1996); CHEN and WU (1996); Zhong and Xiang (2011); Xiang and Liang (2012); Xiang et al. (2013)].

The objective of this paper is to develop a simple, validity and accurate numerical approach for static, free vibration and buckling analysis of FG beam. The governing motion equations of FG beam are derived by using Timoshenko beam theory and Hamilton's principle. This paper is organized as follows. The functionally graded materials are introduced briefly in section 2. The formulation of FGM BSWI beam element is derived in section 3. The numerical results and discussions are shown in section 4. The conclusions are in section 5.

2 Functionally graded materials

A straight uniform functionally graded simply-supported beam with rectangular cross-section is illustrated in Fig.1. L, b and h are the length, width and thickness of FG beam, respectively. A Cartesian co-ordinate system is defined on the left side of FG beam where X-axis is taken along the length direction, Y-axis in the width direction and Z-axis in the thickness direction.

In this study, it is assumed that the material properties of FG beam, such as Young's modulus and mass density, vary continuously throughout the thickness direction according to power law form in terms of volume fraction of material constituents. The power form introduced by Wakashima [Wakashima et al. (1990)] can be expressed

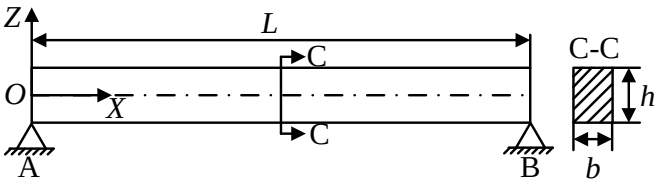

Figure 1: A straight uniform functionally graded simply-supported beam.

as:

$$P(z) = (P_t - P_b)\left(\frac{2z+h}{2h}\right)^n + P_b \tag{1}$$

in which P_t and P_b denote the value of corresponding material properties at the top and bottom of FG beam, respectively, and n is volume fraction exponent which is non-negative. The volume fraction exponent dictates the material variation profile thickness of FG beam.

The material properties of metal-ceramics beam is shown in Fig. 2 to clarify the variation of Young's modulus and mass density throughout the thickness of FG beam with various volume fraction exponents. It is clearly that the bottom ($z/h = -0.5$) material is pure metal (Aluminum) and the top (z/h= 0.5) is pure ceramics (Alumina). The material properties vary continuously throughout the thickness direction with various volume fraction exponents. Moreover, the beam is fully metal and ceramics for n= 0 and $n = \infty$ and the composition of FG beam is linear for n= 1.

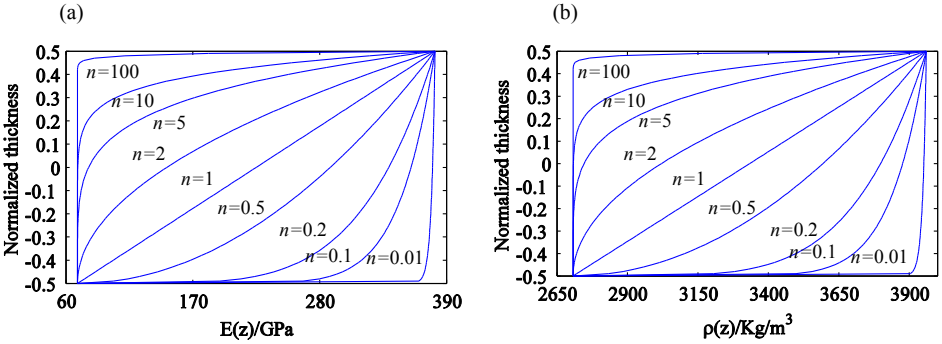

Figure 2: The variation of material properties of metal-ceramics beam with various volume fraction exponents: (a) Young's modulus, (b) mass density.

3 The formulation of FGM BSWI element

3.1 The Timoshenko beam theory and formulations

The Timoshenko beam theory assumes the deformed cross-section planes remain plane but not normal to the middle axis. Based on the theory, the axial displacement u and the transverse displacement w of any point of beam are defined as:

$$u(x,z,t) = u_0(x,t) - z\frac{\partial w_0(x,t)}{\partial x} + z\gamma_0(x,t) \tag{2}$$

$$w(x,z,t) = w_0(x,t) \tag{3}$$

in which u_0 and w_0 are the axial and transverse displacement of the beam on neutral axis, t denotes time and γ_0 is the transverse shear strain of the beam on neutral axis which is given by:

$$\gamma_0(x,t) = \frac{\partial w_0(x,t)}{\partial x} - \theta_0(x,t) \tag{4}$$

in which θ_0 denotes the rotation of the cross-section plane on neutral axis.

Based on small deformations assumption, the normal ε_{xx} and transverse shear γ_{xz} strains can be defined as:

$$\varepsilon_{xx} = \frac{\partial u}{\partial x} = \frac{\partial u_0(x,t)}{\partial x} - z\frac{\partial \theta_0(x,t)}{\partial x} \tag{5}$$

$$\gamma_{xz} = \frac{\partial u}{\partial z} + \frac{\partial w}{\partial x} = \frac{\partial w_0(x,t)}{\partial x} - \theta_0 \tag{6}$$

Considering the transverse shear strain, the total strain energy of beam consists of bending and shear parts:

$$U = U_\varepsilon + U_\gamma \tag{7}$$

in which

$$U_\varepsilon = \frac{1}{2}\int_V \sigma_{xx}\varepsilon_{xx}dV \tag{8}$$

$$U_\gamma = \frac{1}{2}\int_V \tau_{xz}\gamma_{xz}dV \tag{9}$$

in which the normal stress σ_{xx} and transverse shear stress τ_{xz} are obtained according to Hooke's law:

$$\sigma_{xx} = E(z)\varepsilon_{xx} \tag{10}$$

$$\tau_{xz} = kG(z)\gamma_{xz} \tag{11}$$

in which $E(z)$ is the Young' modulus of FG beam varying continuously throughout the thickness direction and $G(z)$ is the shear modulus written as $G(z) = E(z)/2(1+\nu)$. The variable ν is Poisson's ratio and k is the shear correction factor. This factor is always dependent on the cross-section and on the type of problems. The shear correction factor k= 5/6 is frequently adopted for rectangular section.

In this problem, the kinetic energy consists of two parts. Then the kinetic energy can be written as:

$$T = \frac{1}{2}\int_V \rho(z)\left(\frac{\partial u}{\partial t}\right)^2 \mathrm{d}V + \frac{1}{2}\int_V \rho(z)\left(\frac{\partial w}{\partial t}\right)^2 \mathrm{d}V \tag{12}$$

in which $\rho(z)$ denotes the mass density of FG beam varying continuously throughout the thickness direction.

The work done by the external loads acting on the FG beam W can be expressed as:

$$W = \int_0^L (q(x)w + f(x)u)dx + \sum_j F_j w(x_j) + \sum_k M_k \theta(x_k) \tag{13}$$

in which $q(x)$ is the distributed transverse load, $f(x)$ is the distributed axial load, F_j is the concentrated load and M_k is the concentrated bending moment, x_j and x_k stand for the acting locations of concentrated load and moment, respectively.

The total energy of FG beam is formulated as follows:

$$\Pi = U - T - W \tag{14}$$

By aid of the Hamilton's principle, the governing motion equation for static analysis of FG beam can be expressed as:

$$\delta\Pi = \int_{t_1}^{t_2} (\delta U - \delta W)\,\mathrm{d}t = 0 \tag{15}$$

By aid of the Hamilton's principle, the governing motion equation for free vibration analysis of FG beam can be expressed as:

$$\delta\Pi = \int_{t_1}^{t_2} (\delta U - \delta T)\,\mathrm{d}t = 0 \tag{16}$$

3.2 Formulation of FGM BSWI beam element

The FGM BSWI element is constructed through B-spline wavelet on the interval (BSWI) basis to transform the wavelet coefficients space to physical degree space. The j scale mth order BSWI (written as BSWIm_j) scaling functions $\varphi^j_{m,k}(\xi)$ can be evaluated by the following formula [Xiang et al. (2007)]:

$$\varphi^j_{m,k}(\xi)=\begin{cases}\varphi^l_{m,k}(2^{j-l}\xi)\ , k=-m+1,\cdots,-1 \text{ (0 boundary scaling functions)}\\ \varphi^l_{m,2^j-m-k}(1-2^{j-l}\xi)\ , k=2^j-m+1,\cdots,2^j-1 \quad \text{(1 boundary scaling functions)}\\ \varphi^l_{m,0}(2^{j-l}\xi-2^{-l}k),\ k=0,\cdots,2^j-m \quad \text{(inner scaling functions)}\end{cases} \tag{17}$$

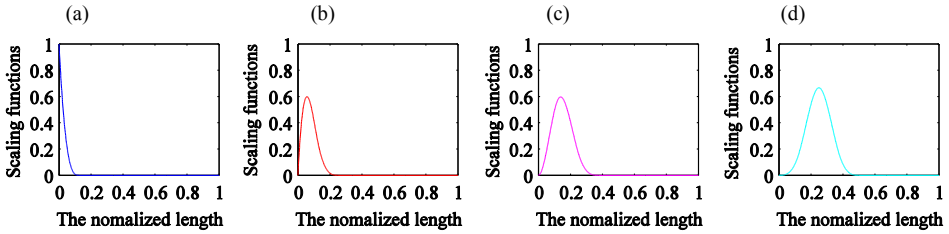

Figure 3: The representative BSWI scaling functions for m=4: (a) k_s = -3, (b) k_s= -2, (c) k_s = -1, (d) k_s =0.

There are m-1 boundary scaling functions at 0 and 1, and 2^j-m+ 1 inner scaling functions. Fig. 3 shows the representative BSWI scaling functions for m = 4 at the scale j = 3. The scaling functions on the interval [0, 1] can be written in vector form [Jiawei et al. (2008)]:

$$\mathbf{\Phi}=\left\{\varphi^j_{m,-m+1}(\xi),\varphi^j_{m,-m+2}(\xi),\cdots,\varphi^j_{m,2^j-1}(\xi)\right\} \tag{18}$$

According to Timoshenko beam theory, the axial displacement, transverse displacement and rotation can be interpolated by BSWI scaling functions, respectively. So the displacement fields are derived as follows:

$$u=\mathbf{\Phi T u}\quad w=\mathbf{\Phi T w}\quad \theta=\mathbf{\Phi T}\boldsymbol{\theta} \tag{19}$$

in which $\mathbf{T}=[\mathbf{\Phi}^T(\xi_1)\ \ \mathbf{\Phi}^T(\xi_2)\ \cdots\ \mathbf{\Phi}^T(\xi_{n+1})]^{-T}$ is the BSWI element transform matrix and $\mathbf{u}$, $\mathbf{w}$, $\boldsymbol{\theta}$ are the displacement vectors in BSWI scaling space, respectively. The element displacement fields can be transformed from wavelet space to

physical space using this transform matrix. Substitute the displacement fields Eq. (19) into Eqs. (5-6) and the results are:

$$\varepsilon_{xx} = \begin{bmatrix} \dfrac{\partial}{\partial x} & 0 & -z\dfrac{\partial}{\partial x} \end{bmatrix} \mathbf{d} \tag{20}$$

$$\gamma_{xz} = \begin{bmatrix} 0 & \dfrac{\partial}{\partial x} & -1 \end{bmatrix} \mathbf{d} \tag{21}$$

in which $\mathbf{d}$ can be expressed as $\mathbf{d} = [u \quad w \quad \theta]^T$.

3.2.1 Static analysis

Substitute Eqs. (20-21) into Eq. 15, the basic governing equation of static problem is derived as

$$\mathbf{K}\mathbf{d} = \mathbf{p} \tag{22}$$

The stiffness matrix $\mathbf{K}$ is defined by the summation of two parts:

$$\mathbf{K} = \mathbf{K}_\varepsilon + \mathbf{K}_\gamma \tag{23}$$

$$\mathbf{K}_\varepsilon = \begin{bmatrix} \mathbf{K}_\varepsilon^{11} & \mathbf{0} & \mathbf{K}_\varepsilon^{13} \\ \mathbf{0} & \mathbf{0} & \mathbf{0} \\ \mathbf{K}_\varepsilon^{31} & \mathbf{0} & \mathbf{K}_\varepsilon^{33} \end{bmatrix} \tag{24}$$

with

$$\mathbf{K}_\varepsilon^{11} = A_1 \times \mathbf{\Gamma}_1^{1,1}, \quad \mathbf{K}_\varepsilon^{13} = A_2 \times \mathbf{\Gamma}_1^{1,1}, \quad \mathbf{K}_\varepsilon^{31} = \mathbf{K}_\varepsilon^{13}, \quad \mathbf{K}_\varepsilon^{33} = A_3 \times \mathbf{\Gamma}_1^{1,1} \tag{25}$$

$$\{A_1, A_2, A_3\} = \int_{-h/2}^{h/2} bE(z)\{1, -z, z^2\}\mathrm{d}z \tag{26}$$

in which the details of integration matrix $\mathbf{\Gamma}$ can be found in **Appendix**.

$$\mathbf{K}_\gamma = \begin{bmatrix} \mathbf{0} & \mathbf{0} & \mathbf{0} \\ \mathbf{0} & \mathbf{K}_\gamma^{22} & \mathbf{K}_\gamma^{23} \\ \mathbf{0} & \mathbf{K}_\gamma^{32} & \mathbf{K}_\gamma^{33} \end{bmatrix} \tag{27}$$

with

$$\mathbf{K}_\gamma^{22} = B_1 \times \mathbf{\Gamma}_1^{1,1}, \quad \mathbf{K}_\gamma^{23} = B_2 \times \mathbf{\Gamma}_1^{1,0}, \quad \mathbf{K}_\gamma^{32} = B_2 \times \mathbf{\Gamma}_1^{0,1}, \quad \mathbf{K}_\gamma^{33} = B_1 \times \mathbf{\Gamma}_1^{0,0} \tag{28}$$

$$\{B_1, B_2\} = \int_{-h/2}^{h/2} kbG(z)\{1, -1\}\mathrm{d}z \tag{29}$$

and the force vector $\mathbf{p}$ can be expressed as:

$$\mathbf{p} = \mathbf{p}_w^e + \mathbf{p}_{w_j}^e + \mathbf{p}_{\theta_k}^e \tag{30}$$

with

$$\mathbf{p}_w^e = \mathbf{T}^T l_e \int_0^1 (q(\xi)\mathbf{\Phi}^T + f(\xi)\mathbf{\Phi}^T)\mathrm{d}\xi \tag{31}$$

$$\mathbf{p}_{w_j}^e = \sum F_j \mathbf{T}^T \mathbf{\Phi}^T(\xi_j) \tag{32}$$

$$\mathbf{p}_{\theta_k}^e = \sum M_k \mathbf{T}^T \mathbf{\Phi}^T(\xi_k) \tag{33}$$

3.2.2 Free vibration analysis

Substitute Eqs. (20-21) into Eq. 16, the basic governing equation of free vibration problem is derived as:

$$(\mathbf{K} - \omega^2 \mathbf{M})\mathbf{X} = \mathbf{0} \tag{34}$$

in which ω is the natural frequency and $\mathbf{X}$ the mode of FG beam. The stiffness matrix $\mathbf{K}$ has been obtained in 3.2.1. The formulation of mass matrix $\mathbf{M}$ is:

$$\mathbf{M} = \begin{bmatrix} \mathbf{M}^{11} & \mathbf{0} & \mathbf{M}^{13} \\ \mathbf{0} & \mathbf{M}^{22} & \mathbf{0} \\ \mathbf{M}^{31} & \mathbf{0} & \mathbf{M}^{33} \end{bmatrix} \tag{35}$$

with

$$\mathbf{M}^{11} = C_1 \times \mathbf{\Gamma}_1^{0,0}, \quad \mathbf{M}^{13} = C_2 \times \mathbf{\Gamma}_1^{0,0}, \quad \mathbf{M}^{22} = \mathbf{M}^{11}, \quad \mathbf{M}^{31} = \mathbf{M}^{13}, \quad \mathbf{M}^{33} = C_3 \times \mathbf{\Gamma}_1^{0,0} \tag{36}$$

$$\{C_1, C_2, C_3\} = \int_{-h/2}^{h/2} b\rho(z)\{1, -z, z^2\}\mathrm{dz} \tag{37}$$

3.2.3 Bucking analysis

The buckling analysis of FG beam involves the solution of eigenvalue problem:

$$(\mathbf{K} - \lambda \mathbf{K}_G)\mathbf{X} = \mathbf{0} \tag{38}$$

in which λ is the critical load and $\mathbf{X}$ the buckling mode of FG beam. The geometric stiffness matrix $\mathbf{K}_G$ is obtained as [Petyt (1990)]:

$$\mathbf{K}_G = p \times \mathbf{\Gamma}_1^{1,1} \tag{39}$$

4 Numerical results and discussions

The FGM BSWI element for the static, free vibration and buckling analysis of FG beam according to Timoshenko beam theory and Hamilton's principle has been formulated in preceding sections. In this section, various numerical examples are presented and discussed to demonstrate the validity, high convergence and accuracy of the proposed element. First of all, some parameters will be explained. In practice, Poisson's ratio commonly varies slightly. Therefore, v is taken as a constant throughout the thickness direction of FG beam. The shear correction factor k is taken as 5/6 for rectangular section.

4.1 Static analysis of FG beam

In this section, the static analysis of FG beam is investigated with two numerical examples. The first example is concerned with a homogeneous beam to demonstrate the accuracy and fast convergence of the proposed FGM BSWI element for static analysis. And the second example is concerned with a FG beam with various volume fraction exponents for different length-to-height ratios. These numerical examples demonstrate that the proposed FGM BSWI element is validity, accurate and fast convergence for static analysis of FG beam.

4.1.1 Accuracy and convergence of BSWI method for static analysis

The homogeneous beam can be considered as a special class of FG beam with volume fraction exponent $n = 0$. Therefore, the FG beam with $n= 0$ is employed for comprehensive comparison. In this example, the material properties are constant throughout the thickness of FG beam. The referential solutions for cantilever and simply-supported homogeneous beam have been calculated by Heyliger [Heyliger and Reddy (1988)] and the exact solutions for the same problems have also been provided by Bickford [Bickford (1982)]. The cantilevered beam under an end load F and simply-supported beam under a uniform load q are considered. Heyliger [Heyliger and Reddy (1988)] has solved for several values of L with $h= 12$, $b= 1$, $E= 29000$, $v= 0.3$, $F= 100$ and $q= 10$ in Table 1. The difference, the following expression is used for percents: (Referential solutions - Exact)/Exact $\times$ 100%, between the maximum deflection of the solutions with exact solutions is drawn in Fig. 4. It is observed from Fig. 4. that the proposed FGM BSWI element achieves an excellent agreement with the referential solutions in $N = 16$ and the exact solutions for different boundary conditions and length-to-height ratios. The difference between the present method and exact is almost zero. The validity, accuracy and fast convergence of proposed FGM BSWI element have also been demonstrated with the aid of only one FGM BSWI element. In addition, one FGM BSWI element is adopted in the following examples if no explanation is given.

Table 1: The maximum deflections of FG beam (n = 0).

Boundary	Length(L)	Finite element solution [Heyliger and Reddy (1988)]				Exact [Bickford (1982)]	Present
		N=2	N=4	N=8	N=16		
C-F	160	30.838	32.368	32.742	32.823	32.838	32.838
	80	3.9234	4.1105	4.1506	4.1567	4.1585	4.1586
	40	0.52266	0.54249	0.54540	0.54588	0.54668	0.54671
	12	0.023551	0.023741	0.023874	0.023931	0.024518	0.024551
S-S	160	19.779	20.529	20.691	20.717	20.721	20.721
	80	1.3011	1.3415	1.3478	1.3486	1.3488	1.3489
	40	9.603×10^{-2}	9.774×10^{-2}	9.777×10^{-2}	9.770×10^{-2}	9.771×10^{-2}	9.775×10^{-2}
	12	2.223×10^{-3}	2.221×10^{-3}	2.220×10^{-3}	2.220×10^{-3}	2.220×10^{-3}	2.220×10^{-3}

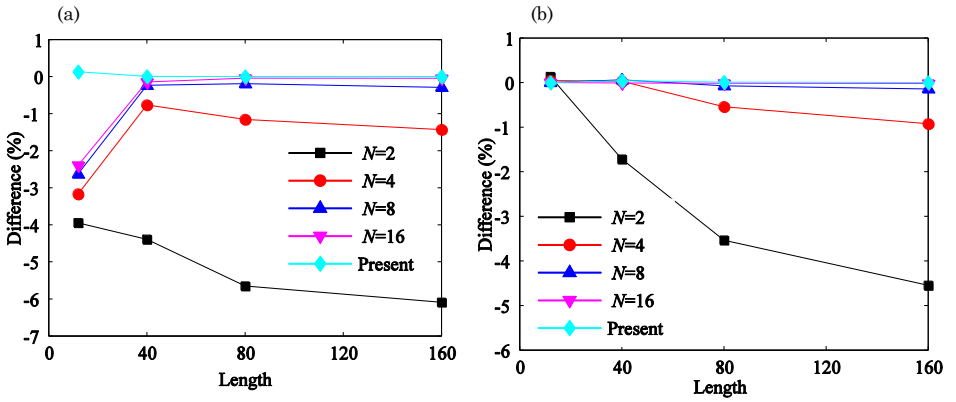

Figure 4: The difference between the maximum deflections of different methods (a) C-F (b) S-S.

4.1.2 Effect of volume fraction exponent

In Table 2, the maximum normalized transverse deflections of the simply-supported FG beam are given for various volume fraction exponents. The FG beam is composed of two materials with the top material being pure aluminum (E_m= 70 GPa) and the bottom material being pure zirconia (E_c= 200 GPa). The cross section is $b \times h$= 0.1 m×0.1 m and the length is taken as L= 0.4 m and L= 1.6 m. The transverse displacements of FG beam is normalized as:

$$w_{static} = 5qL^4/384E_mI \tag{40}$$

For this problem, the referential solutions given by Şimşek [Şimşek (2009)] using Timoshenko beam theory (FSDBT) and higher order shear deformation beam theory (HSDBT) are used for comparison. Based on one BSWI element, an excellent agreement between the present BSWI method and referential solutions, especially for slender beam, is achieved in Table 2. It seems the solutions given by present method are not compared well for thick beam (L/h = 4). Considering the higher terms, the HSDBT method can obtain more accurate solutions than FSDBT for thick beam. The effect of transverse shear deformation becomes weak with the increasing length-to-height ratio of beam. Thus, the differences between the HSDBT and FSDBT method become smaller for slender beam (L/h = 16). Although the HSDBT method presents better solutions for thick and slender beam, their equations are much more complicated than those of FSDBT. And solutions in table 2 show that the FGM BSWI element formulated by FSDBT could give satisfactory results and it is very effective to investigate behavior of FG beam. Therefore, the simple

Table 2: The maximum normalized transverse deflections of FG beam with various volume fraction exponents.

L/h	Theory	Maximum normalized transverse deflection						
		Full metal	n =0.2	n =0.5	n =1	n =2	n=5	Full ceramic
4	FSDBT [Şimşek (2009)]	1.13002	0.84906	0.71482	0.62936	0.56165	0.49176	0.39550
	HSDBT [Şimşek (2009)]	1.15578	0.87145	0.73264	0.64271	0.57142	0.49978	0.40452
	Present	1.15600	0.86846	0.73080	0.64283	0.57326	0.50196	0.40460
16	FSDBT [Şimşek (2009)]	1.00812	0.75595	0.63953	0.56615	0.50718	0.44391	0.35284
	HSDBT [Şimşek (2009)]	1.00975	0.75737	0.64065	0.56699	0.50780	0.44442	0.35341
	Present	1.00975	0.75678	0.64047	0.56700	0.50791	0.44455	0.35341

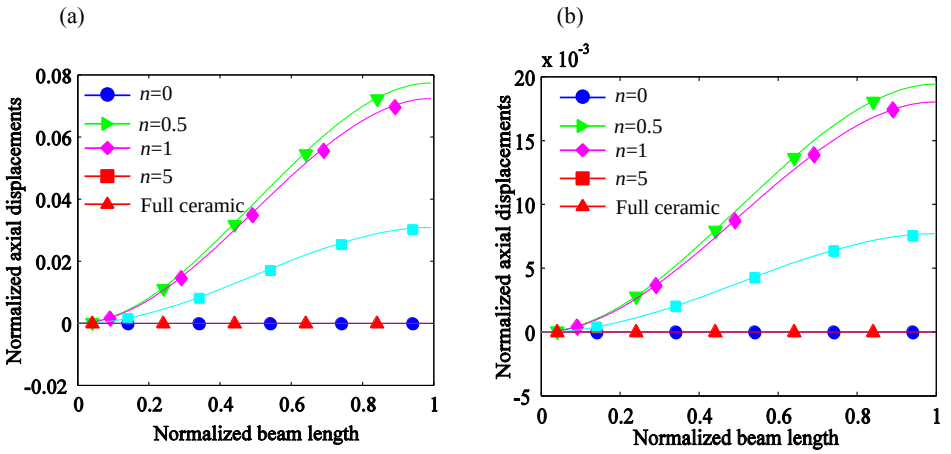

Figure 5: The normalized axial displacements of FG beam along the length direction: (a) L/h=4 (b) L/h=16.

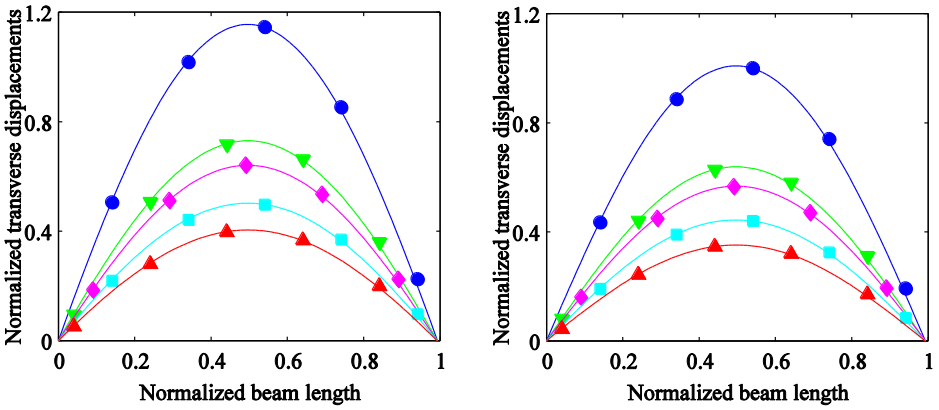

Figure 6: The normalized transverse displacements of FG beam along the length direction (a) L/h=4 (b) L/h=16 (the legends are the same with Fig. 5.).

but accurate FSDBT is employed for the formulation of FG BSWI element. Fig. 5-6 show the normalized axial and transverse displacements of FG beam for L=0.4 m and L=1.6 m, respectively. There is coupling between the bending (displacement on z) and the stretching (displacement on x) for FG beam. The coupling is caused by the material properties varying continuously throughout the thickness direction of FG beam. While the material properties of homogeneous beam (n=0 or ∞) are constant, the bending and stretching of homogeneous beam are uncoupling. What's

more, the axial and transverse displacements decrease as volume fraction exponent increases. The reason must be the full metal beam ($n = 0$) has the minimum bending stiffness and bending stiffness increases gradually as volume fraction exponent increases.

4.2 Free vibration analysis of FG beam

In this section, the free vibration analysis of FG beam is investigated with four numerical examples. The first example is concerned with a homogeneous beam to demonstrate the accuracy and fast convergence of the proposed FGM BSWI element for vibration analysis. The second example is concerned with FG beam with the first five natural frequencies and then the following two examples are concerned with FG beam with different boundary conditions and volume fraction exponents for different length-to-height ratios. These numerical examples demonstrate that the proposed FGM BSWI element is validity, accurate and fast convergence for free vibration analysis of FG beam.

4.2.1 Accuracy and convergence of BSWI method for free vibration analysis

Firstly, a FG beam with volume fraction exponent n= 0 is employed for comprehensive comparison. In this example, the material properties are constant throughout the thickness of FG beam. The exact natural frequencies for a homogenous beam have been given by Timoshenko [Timoshenko (1974)] and the referential solutions for a cantilever homogeneous beam have also been calculated by Li [Huang and Li (2010)]. The normalized natural frequency is defined as:

$$\bar{\omega} = \omega L^2 \sqrt{\rho A / EI} \tag{41}$$

The first four normalized natural frequencies calculated by the FGM BSWI element are tabulated in Table 3 compared with the exact solutions and other referential results. The difference, the following expression is used for percents: (Referential solutions - Exact)/Exact $\times$ 100%, between the first four frequencies of the solutions with exact solutions is drawn in Fig. 7. Observing from Fig. 7, the present method has a great agreement with the exact solutions [Timoshenko (1974)] and referential solutions with N= 10 obtained by Li [Huang and Li (2010)]. The tiny error is mainly caused by one FGM BSWI element with only eleven nodes used to investigate in this problem. The comparison results demonstrate that the present FGM BSWI element is very accurate and fast convergence for free vibration problem of beam.

4.2.2 Effect of mode number

Another comparison for the first five natural frequencies of a pinned-pinned FG beam is presented in Table 4. The FG beam is made of steel and aluminum with

Table 3: The first four normalized natural frequencies of cantilever FG beam (n = 0).

Mode number	Referential solutions [Huang and Li (2010)]				Exact [Timoshenko (1974)]	Present
	N=2	N=4	N=6	N=10		
1	3.5171	3.5160	3.5160	3.5160	3.5160	3.5160
2	22.2334	22.0351	22.0345	22.0345	22.0345	22.0339
3	118.1444	63.2397	61.7151	61.6972	61.6972	61.6946
4	-	128.5194	121.1184	120.9019	120.9019	120.9004

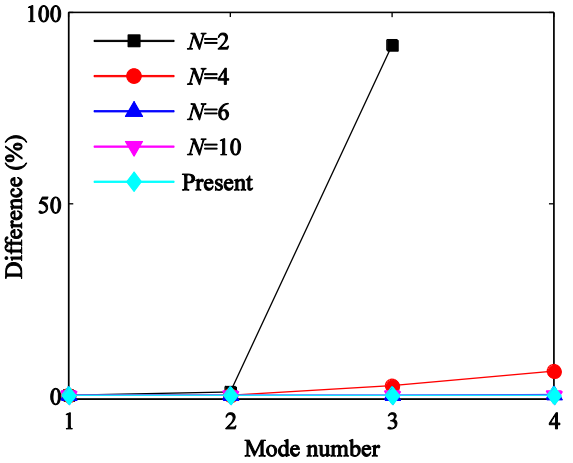

Figure 7: The difference between the first four frequencies of different methods.

n=1. The material properties are E_{steel}= 210 GPa, ρ_{steel}= 7850 kg/m^3, E_{Al}= 70 GPa, ρ_{Al}= 2707 kg/m^3,ν_{steel}= ν_{Al}= 0.3 and the cross section is $L \times h$ = 0.5 m$\times$0.125 m. For this problem, the referential solutions have been obtained by Li [Li (2008)] based on the first order shear deformation beam theory (FSDBT), and other referential solutions were also given by Şimşek [Şimşek (2010a)] using the first order (FSDBT) and different higher-order shear deformation beam theories (HSDBTs). The difference, the following expression is used for percents: (Referential solutions-Li(2008))/ Li(2008) $\times$100%, between the first five frequencies of these solutions with Li [Li (2008)] is drawn in Fig. 8. Observing from Fig. 8., the results presented by FGM BSWI element show a good agreement with the results of Li [Li (2008)] and Şimşek [Şimşek (2010a)] in the lower mode shapes. The agreement becomes weak for the higher frequencies, especially for the fifth frequency. However, the

maximum difference is less than 1% for the fifth frequency. This phenomenon is caused by the fewer degrees of freedoms used in BSWI for calculating frequencies. It can be concluded that the error for higher frequencies can be eliminated with the increasing degrees of freedoms. Fig. 9 shows the corresponding first three mode shapes of FG beam.

Table 4: The first five natural frequencies of pinned-pinned FG beam (n=1).

Mode number	Natural frequency(rad/s)					
	FSDBT*	PSDBT*	ESDBT*	ASDBT*	Li [Li (2008)]	Present
1	6443.08	6443.78	6446.42	6446.42	6457.93	6457.92
2	21470.95	21493.99	21525.48	21525.48	21603.18	21603.53
3	39775.55	39909.87	40,031.20	40031.20	40145.42	40153.20
4	59092.37	59509.80	59813.79	59813.79	59779.01	59854.79
5	78638.36	79589.32	80196.95	80196.95	79686.16	80156.67
* denotes the solutions given by Şimşek [Şimşek (2010a)]						

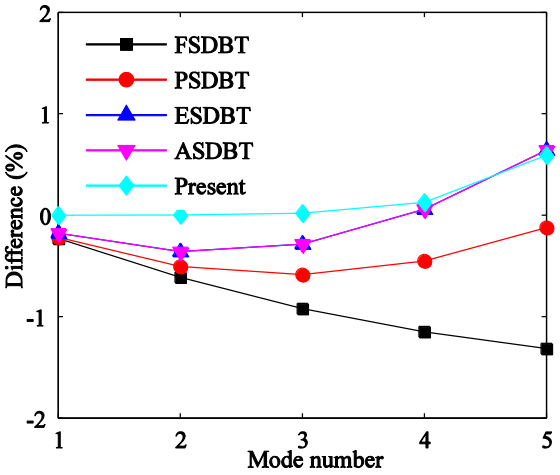

Figure 8: The difference between the first five frequencies of different methods.

4.2.3 *Effect of boundary condition*

Further comparison for the normalized natural frequencies of FG beam subjected to different boundary conditions with different length-to-height ratios is presented in Table 5. The FG beam is composed of aluminum and alumina and the material

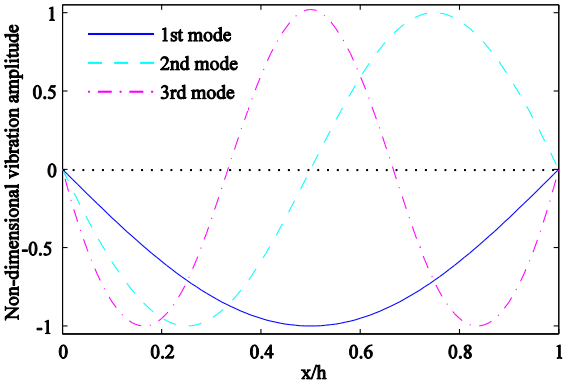

Figure 9: The first three mode shapes of FG beam.

properties are: aluminum for E_b= 70 GPa, ρ_b = 2702 kg/m^3, v_b= 0.3 and alumina for E_u= 380 GPa, ρ_u= 3960 kg/m^3, v_u= 0.3

Table 5: The normalized fundamental frequencies of FG beam (n=0.3).

Boundary	L/h	10	30	100
S-S	FSDBT1 [Sina et al. (2009)]	2.774	2.813	2.817
	FSDBT2 [Sina et al. (2009)]	2.695	2.737	2.742
	Present	2.735	2.774	2.778
C-F	FSDBT1 [Sina et al. (2009)]	0.996	1.003	1.003
	FSDBT2 [Sina et al. (2009)]	0.969	0.976	0.977
	Present	0.970	0.976	0.977
C-C	FSDBT1 [Sina et al. (2009)]	6.013	6.343	6.384
	FSDBT2 [Sina et al. (2009)]	5.811	6.167	6.212
	Present	5.852	6.174	6.223

The normalized frequency form is used as:

$$\hat{\omega} = \omega L^2 \sqrt{I/h^2 / \int_{-h/2}^{h/2} E \mathrm{d}z} \tag{42}$$

The normalized fundamental frequencies of FG beam with simply-simply (S-S), clamp-free (C-F) and clamp-clamp (C-C) boundary conditions are researched and obtained for different length-to-height ratios, L/h= 10, L/h= 30 and L/h= 100, by

Sina [Sina et al. (2009)]. It is clear that the solutions obtained by the present method are in good agreement with the FSDBT2 solutions, especially for the C-F and C-C boundary conditions. Fig. 10 shows the mode shapes of FG beam with different length-to-height ratios for different boundary conditions. It is observed that the solving mode shapes are very consistent with the real vibration of beam which verifies the correctness of the proposed FGM BSWI element once more.

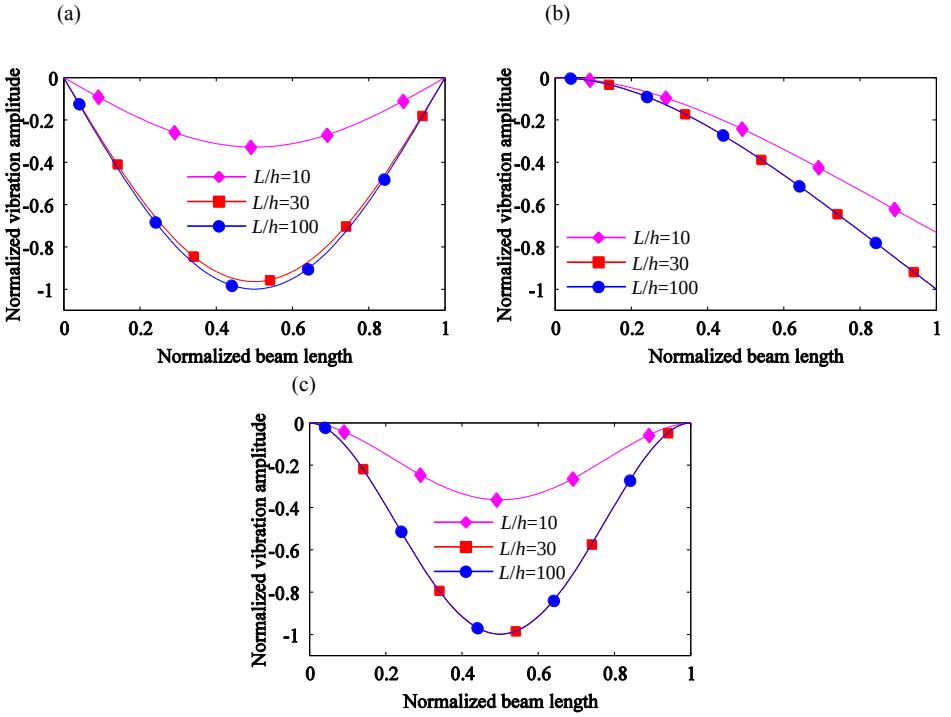

Figure 10: The mode shapes of FG beam with different length-to-height ratios for different boundary conditions: (a) S-S, (b) C-F, (c) C-C.

4.2.4 *Effect of volume fraction exponent*

The final comparison for the normalized natural frequencies of FG beam with various volume fraction exponents is presented in Table 6. The materials of FG beam are the same with those in 4.2.3. The normalized natural frequency form is expressed as:

$$\tilde{\omega} = \omega L^2 \sqrt{\rho_b / E_b} / h \tag{43}$$

The calculated first three normalized frequencies of FG beam for various volume fraction exponents are compared with those solutions given by Thai [Thai and Vo (2012)] using the third-order beam theory. The beam is simply-supported and the length-to-height ratios are L/h=5, L/h=20. It is observed from Table 6 that the present results are in good agreement with the results of Thai [Thai and Vo (2012)], especially for larger length-to-height ratio. Fig. 11 shows the first three normalized natural frequencies for different length-to-height ratios and volume fraction exponents.

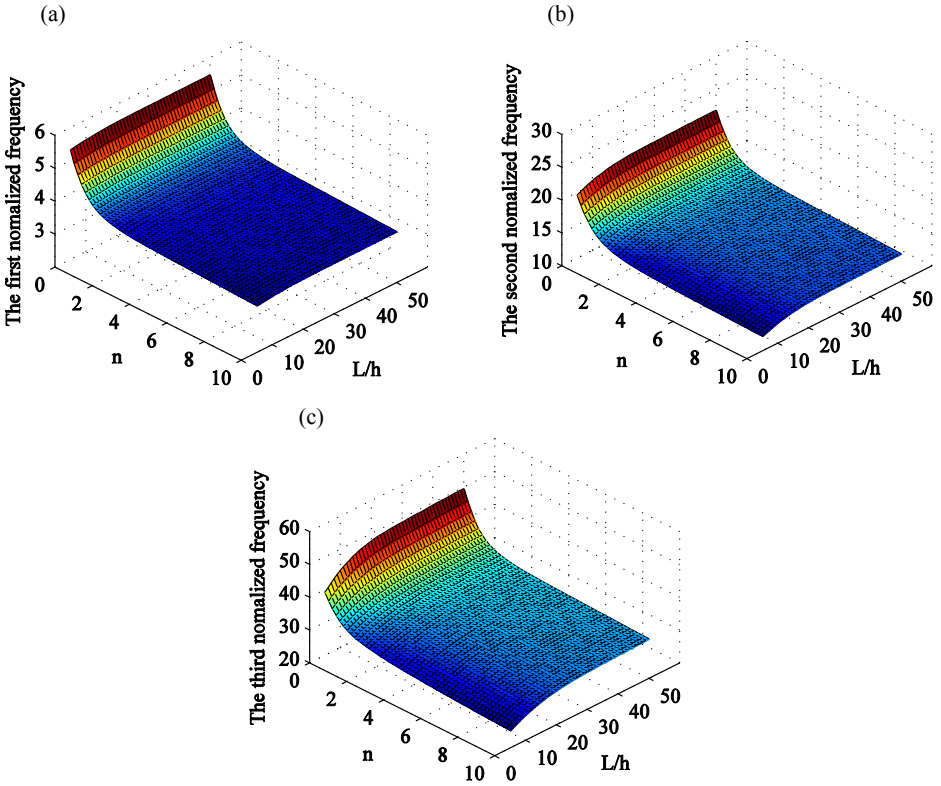

Figure 11: The first three normalized natural frequencies of FG beam with different length-to-height ratios and volume fraction exponents. (a) the first normalized natural frequency, (b) the second normalized natural frequency, (c) the third normalized natural frequency.

Table 6: The first three normalized natural frequencies of simply-supported FG beam.

L/h	Mode	Method	Normalized natural frequencies					
			$n = 0$	$n = 0.5$	$n = 1$	$n = 2$	$n = 5$	$n = 10$
5	1	Thai [Thai and Vo (2012)]	5.1527	4.4107	3.9904	3.6264	3.4012	3.2816
		Present	5.1525	4.3988	3.9709	3.6047	3.4023	3.2961
	2	Thai [Thai and Vo (2012)]	17.8812	15.4588	14.0100	12.6405	11.5431	11.0240
		Present	17.8711	15.6114	14.4129	13.2401	12.1389	11.4620
	3	Thai [Thai and Vo (2012)]	34.2097	29.8382	27.0979	24.3152	21.7158	20.5561
		Present	34.1449	29.6974	27.0193	24.4456	22.3819	21.2617
20	1	Thai [Thai and Vo (2012)]	5.4603	4.6511	4.2051	3.8361	3.6485	3.5390
		Present	5.4603	4.6503	4.2037	3.8347	3.6488	3.5403
	2	Thai [Thai and Vo (2012)]	21.5732	18.3962	16.6344	15.1619	14.3746	13.9263
		Present	21.5732	18.3824	16.6115	15.1362	14.3758	13.9438
	3	Thai [Thai and Vo (2012)]	47.5930	40.6526	36.7679	33.4689	31.5780	30.5369
		Present	47.5921	40.5450	36.5789	33.2204	31.3956	30.4588

4.3 Buckling analysis of FG beam

In this section, the buckling analysis of FG beam is investigated with two numerical examples. The first example is concerned with a homogeneous beam to demonstrate the accuracy and high convergence of the proposed FGM BSWI element for buckling analysis. The second example is concerned with FG beam with various volume fraction exponents for different length-to-height ratios. These numerical examples demonstrate that the proposed FGM BSWI element is validity, accurate and fast convergence for buckling analysis of FG beam.

4.3.1 Accuracy and convergence of BSWI method for buckling analysis

Firstly, a FG beam with the volume fraction exponent n=0 is employed for comprehensive comparison. In this example, the material properties are constant throughout the thickness of beam. The exact critical loads [Bazant and Cedolin)] for a homogenous beam with pined-pined (P-P) and simply-simply (S-S) boundary conditions are:

$$P_{cr} = k\pi^2 GAEI/(kL_{eff}^2 GA + \pi^2 EI) \tag{44}$$

in which L_{eff} is effective beam length for pinned-pinned beams $L_{eff} = L$ and simply-simply beams $L_{eff} = L/2$. Ferreira [Ferreira (2008)] has given the referential solutions for different length-to-height ratios, L/h= 10, L/h= 100 and L/h= 1000, using 40 traditional finite elements in Table 7. It is seen from Table 7 that the present method can get more accurate results using only one FGM BSWI element and the results are validity, accuracy and fast convergence for different boundary conditions and length-to-height ratios.

Table 7: The critical loads of FG beam (n=0).

Boundary	P-P			S-S		
L/h	Ferrerira [Ferreira (2008)]	Exact [Bazant and Cedolin)]	Present	Ferrerira [Ferreira (2008)]	Exact [Bazant and Cedolin)]	Present
10	8021.8	8013.8	8015.4	29877	29766	29766
100	8.231	8.223	8.224	32.999	32.864	32.864
1000	0.0082	0.0082	0.0082	0.0330	0.0329	0.0329

4.3.2 Effect of boundary condition and volume fraction exponent

Further comparison for the normalized critical loads of FG beam subjected to different boundary conditions with different length-to-height ratios is presented in

Table 8. The FG beam is assumed to be composed of metal (aluminum) and ceramic (alumina) and the Young' modulus of materials are the same with 4.2.3 and the passion's ratio is v=0.23. The normalized critical load form is expressed as:

$$\lambda = P_{\mathrm{cr}} L^2/(E_b I) \tag{45}$$

The present results are compared with the solutions given by Batra [Li and Batra (2013)] using the Timoshenko beam theory. From Table 8, it is observed that the present results are in great agreement with the solutions obtained by Batra [Li and Batra (2013)] and the results prove that the formulated FGM BSWI element is very suitable and accuracy for calculating the critical loads of FG beam for various boundary conditions and length-to-height ratios. Fig. 12 shows the first three buckling mode shapes for different boundaries conditions. It is also observed that the solving buckling mode shapes are very consistent with the real buckling mode shapes of homogeneous beam.

Table 8: The normalized critical loads of FG beam.

L/h	Boundary	Normalized critical loads							
		n=0	n=0.5	n=1	n=2	n=5	n=10	n=100	n=10^{11}
5	C-C	154.35[a]	103.22	80.498	62.614	50.384	44.267	31.231	28.433
		154.33[b]	103.21	80.490	62.608	50.378	44.262	31.227	28.430
	S-S	48.835[a]	31.967	24.687	19.245	16.024	14.427	10.020	8.9959
		48.833[b]	31.966	24.686	19.244	16.023	14.427	10.020	8.9956
	C-F	13.213[a]	8.5782	6.6002	5.1495	4.3445	3.9501	2.7563	2.4340
		13.077[b]	8.4991	6.5426	5.1040	4.2984	3.9030	2.6960	2.4089
10	C-C	195.34[a]	127.87	98.749	76.980	64.096	57.708	40.081	35.984
		195.33[b]	127.86	98.745	76.978	64.094	57.706	40.080	35.983
	S-S	52.309[a]	33.996	26.171	20.416	17.192	15.612	10.784	9.6357
		52.307[b]	33.996	26.170	20.416	17.194	15.612	10.784	9.6356
	C-F	13.349[a]	8.6566	6.6570	5.1944	4.3903	3.9969	2.7562	2.4589
		13.314[b]	8.6362	6.6424	5.1828	4.3784	3.9849	2.7485	2.4525
a denotes the solutions given by Batra [Li and Batra (2013)]									
b denotes the solutions given by present method									

5 Conclusions

A new approach has been proposed to solve static, free vibration and buckling problems of FG beam with material properties continuously varying through the thickness direction according to power law form. The governing motion equations

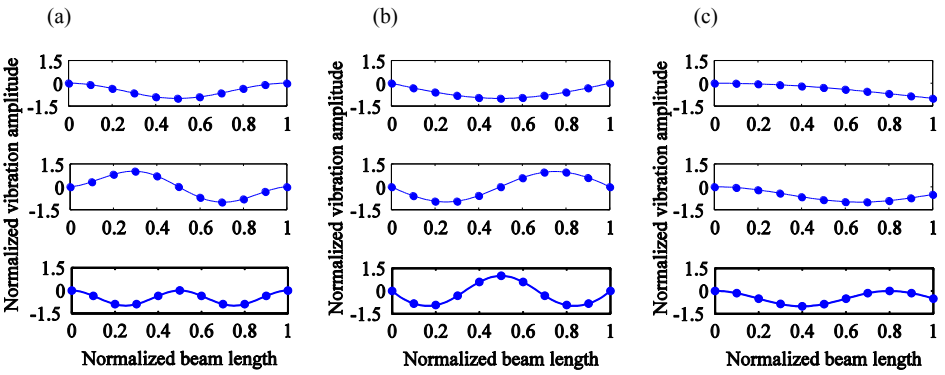

Figure 12: The first three buckling mode shapes of FG beam with different boundary conditions: (a) C-C, (b) S-S, (c) C-F.

of FG beam are derived via the Timoshenko beam theory and Hamilton's principle. In this paper, BSWI scaling function is adopted to form the shape function instead of the polynomial interpolation used in traditional finite element method. Then the corresponding wavelet-based element named FGM BSWI element is constructed for the static, free vibration and buckling analysis of FG beam. The comparisons with different results show that the new approach obtains satisfactory results for the static, free vibration and buckling analysis of FG beam for different boundary conditions comparing with exact solutions and referential solutions existing in literatures. What's more, the validity, accuracy and fast convergence of this approach are also demonstrated. Therefore, the formulated FGM BSWI element is very suitable to investigate the static and dynamic of FG beam which has a board prospect in practical applications.

Acknowledgement: This work was supported by the National Natural Science Foundation of China (Nos. 51405369 & 51175401), the China Postdoctoral Science Foundation (No. 2014M560766), and the Fundamental Research Funds for the Central Universities (No. xjj2014107).

References

Alshorbagy, A. E.; Eltaher, M.; Mahmoud, F. (2011): Free vibration characteristics of a functionally graded beam by finite element method. *Applied Mathematical Modelling,* vol. 35, pp. 412-425.

Atluri, S.; Sladek, J.; Sladek, V.; Zhu, T. (2000): The local boundary integral equation (LBIE) and it's meshless implementation for linear elasticity. *Computa-*

tional mechanics, vol. 25, pp. 180-198.

Atluri, S.; Zhu, T. (1998): A new meshless local Petrov-Galerkin (MLPG) approach in computational mechanics. *Computational mechanics,* vol. 22, pp. 117-127.

Atluri, S. N.; Kim, H.-G.; Cho, J. Y. (1999): A critical assessment of the truly meshless local Petrov-Galerkin (MLPG), and local boundary integral equation (LBIE) methods. *Computational Mechanics,* vol. 24, pp. 348-372.

Atmane, H. A.; Tounsi, A.; Meftah, S. A.; Belhadj, H. A. (2011): Free vibration behavior of exponential functionally graded beams with varying cross-section. *Journal of Vibration and Control,* vol. 17, pp. 311-318.

Aydogdu, M. (2008): Semi-inverse method for vibration and buckling of axially functionally graded beams. *Journal of Reinforced Plastics and Composites,* vol. 27, pp. 683-691.

Aydogdu, M.; Taskin, V. (2007): Free vibration analysis of functionally graded beams with simply supported edges. *Materials & design,* vol. 28, pp. 1651-1656.

Bazant, Z.; Cedolin, L. (1991): *Stability of structures.* Oxford University Press, New York.

Benatta, M.; Mechab, I.; Tounsi, A.; Adda Bedia, E. (2008): Static analysis of functionally graded short beams including warping and shear deformation effects. *Computational Materials Science,* vol. 44, pp. 765-773.

Bickford, W. (1982): A consistent higher order beam theory. *developments in theoretical and Applied Mechanics,* vol. 11, pp. 137-150.

Birman, V.; Byrd, L. W. (2007): Modeling and analysis of functionally graded materials and structures. *Applied Mechanics Reviews,* vol. 60, pp. 195-216.

Chakraborty, A.; Gopalakrishnan, S.; Reddy, J. (2003): A new beam finite element for the analysis of functionally graded materials. *International Journal of Mechanical Sciences,* vol. 45, pp. 519-539.

Chen, W.-H.; Wu, C.-W. (1995): A spline wavelets element method for frame structures vibration. *Computational Mechanics,* vol. 16, pp. 11-21.

Chen, W. H.; Wu, C. W. (1996): Adaptable spline element for membrane vibration analysis. *International journal for numerical methods in engineering,* vol. 39, pp. 2457-2476.

Cohen, A. (2003): *Numerical analysis of wavelet methods*, Elsevier.

Dong, L.; Atluri, S. (2011): A simple procedure to develop efficient & stable hybrid/mixed elements, and Voronoi cell finite elements for macro-& micromechanics. *Computers Materials and Continua,* vol. 24, pp. 61-104.

Dong, L.; El-Gizawy, A. S.; Juhany, K. A.; Atluri, S. N. (2014a): A Simple Locking-Alleviated 3D 8-Node Mixed-Collocation C 0 Finite Element with Over-Integration, for Functionally-Graded and Laminated Thick-Section Plates and Shells, with & without Z-Pins. vol. 41, pp. 163-192.

Dong, L.; El-Gizawy, A. S.; Juhany, K. A.; Atluri, S. N. (2014b): A Simple Locking-Alleviated 4-Node Mixed-Collocation Finite Element with Over-Integration, for Homogeneous or Functionally-Graded or Thick-Section Laminated Composite Beams. *CMC: Computers, Materials & Continua,* vol. 40, pp. 49-77.

Ferreira, A. J. (2008): *MATLAB codes for finite element analysis: solids and structures*, Springer.

Hartmann, R.; Houston, P. (2002): Adaptive discontinuous Galerkin finite element methods for the compressible Euler equations. *Journal of Computational Physics,* vol. 183, pp. 508-532.

Heyliger, P. R.; Reddy, J. N. (1988): A higher order beam finite element for bending and vibration problems. *Journal of sound and vibration,* vol. 126, pp. 309-326.

Huang, Y.; Li, X.-F. (2010): A new approach for free vibration of axially functionally graded beams with non-uniform cross-section. *Journal of Sound and Vibration,* vol. 329, pp. 2291-2303.

Jiawei, X.; Xuefeng, C.; Zhengjia, H.; Yinghong, Z. (2008): A new wavelet-based thin plate element using B-spline wavelet on the interval. *Computational Mechanics,* vol. 41, pp. 243-255.

Kadoli, R.; Akhtar, K.; Ganesan, N. (2008): Static analysis of functionally graded beams using higher order shear deformation theory. *Applied Mathematical Modelling,* vol. 32, pp. 2509-2525.

Kapuria, S.; Bhattacharyya, M.; Kumar, A. (2008): Bending and free vibration response of layered functionally graded beams: a theoretical model and its experimental validation. *Composite Structures,* vol. 82, pp. 390-402.

Koizumi, M. (1993): Concept of FGM. *Ceramic Transactions,* vol. 34, pp. 3-10.

Koizumi, M. (1997): FGM activities in Japan. *Composites Part B: Engineering,* vol. 28, pp. 1-4.

Kosec, G.; Šarler, B. (2011): H-adaptive local radial basis function collocation meshless method. *Computers Materials and Continua,* vol. 26, pp. 227.

Li, S.-R.; Batra, R. C. (2013): Relations between buckling loads of functionally graded Timoshenko and homogeneous Euler–Bernoulli beams. *Composite Structures,* vol. 95, pp. 5-9.

Li, X.-F.; Wang, B.-L.; Han, J.-C. (2010): A higher-order theory for static and

dynamic analyses of functionally graded beams. *Archive of Applied Mechanics,* vol. 80, pp. 1197-1212.

Li, X. F. (2008): A unified approach for analyzing static and dynamic behaviors of functionally graded Timoshenko and Euler–Bernoulli beams. *Journal of Sound and vibration,* vol. 318, pp. 1210-1229.

Mahi, A.; Adda Bedia, E. A.; Tounsi, A.; Mechab, I. (2010): An analytical method for temperature-dependent free vibration analysis of functionally graded beams with general boundary conditions. *Composite Structures,* vol. 92, pp. 1877-1887.

Mazzei, A. J.; Scott, R. A. (2013): On the effects of non-homogeneous materials on the vibrations and static stability of tapered shafts. *Journal of Vibration and Control,* vol. 19, pp. 771-786.

Petyt, M. (1990): *Introduction to finite element vibration analysis.* Cambridge University, Cambridge.

Pradhan, K. K.; Chakraverty, S. (2013): Free vibration of Euler and Timoshenko functionally graded beams by Rayleigh–Ritz method. *Composites Part B: Engineering,* vol. 51, pp. 175-184.

Pradhan, K. K.; Chakraverty, S. (2014): Effects of different shear deformation theories on free vibration of functionally graded beams. *International Journal of Mechanical Sciences,* vol 82, pp. 149-160.

Sankar, B. V. (2001): An elasticity solution for functionally graded beams. *Composites Science and Technology,* vol. 61, pp. 689-696.

Şimşek, M. (2009): Static analysis of a functionally graded beam under a uniformly distributed load by Ritz method. *Int J Eng Appl Sci,* vol. 1, pp. 1-11.

Şimşek, M. (2010a): Fundamental frequency analysis of functionally graded beams by using different higher-order beam theories. *Nuclear Engineering and Design,* vol. 240, pp. 697-705.

Şimşek, M. (2010b): Vibration analysis of a functionally graded beam under a moving mass by using different beam theories. *Composite Structures,* vol. 92, pp. 904-917.

Şimşek, M.; Kocatürk, T. (2009): Free and forced vibration of a functionally graded beam subjected to a concentrated moving harmonic load. *Composite Structures,* vol. 90, pp. 465-473.

Sina, S.; Navazi, H.; Haddadpour, H. (2009): An analytical method for free vibration analysis of functionally graded beams. *Materials & Design,* vol. 30, pp. 741-747.

Suresh, S.; Mortensen, A.; Suresh, S. (1998): *Fundamentals of functionally grad-*

ed materials, Institute of Materials London.

Thai, H.-T.; Vo, T. P. (2012): Bending and free vibration of functionally graded beams using various higher-order shear deformation beam theories. *International Journal of Mechanical Sciences,* vol. 62, pp. 57-66.

Timoshenko, S. (1974): *Vibration problems in engineering.* Wiley, New York.

Viola, E.; Tornabene, F. (2009): Free vibrations of three parameter functionally graded parabolic panels of revolution. *Mechanics research communications,* vol. 36, pp. 587-594.

Wakashima, K.; Hirano, T.; Niino, M. (1990): Space applications of advanced structural materials. *ESA SP,* vol. 303, pp. 97.

Wattanasakulpong, N.; Gangadhara Prusty, B.; Kelly, D. W. (2011): Thermal buckling and elastic vibration of third-order shear deformable functionally graded beams. *International Journal of Mechanical Sciences,* vol. 53, pp. 734-743.

Wu, C.; Chen, W.-H. (1996): Extension of spline wavelets element method to membrane vibration analysis. *Computational mechanics,* vol. 18, pp. 46-54.

Xiang, J.; Chen, X.; He, Z.; Dong, H. (2007): The construction of 1D wavelet finite elements for structural analysis. *Computational Mechanics,* vol. 40, pp. 325-339.

Xiang, J.; Liang, M. (2012): Wavelet-Based Detection of Beam Cracks Using Modal Shape and Frequency Measurements. *Computer-Aided Civil and Infrastructure Engineering,* vol. 27, pp. 439-454.

Xiang, J.; Long, J.; Jiang, Z. (2010): A numerical study using Hermitian cubic spline wavelets for the analysis of shafts. *Proceedings of the Institution of Mechanical Engineers, Part C: Journal of Mechanical Engineering Science,* vol. 224, pp. 1843-1851.

Xiang, J.; Matsumoto, T.; Wang, Y.; Jiang, Z. (2013): Detect damages in conical shells using curvature mode shape and wavelet finite element method. *International Journal of Mechanical Sciences,* vol. 66, pp. 83-93.

Zhang, T.; Dong, L.; Alotaibi, A.; Atluri, S. N. (2013): Application of the MLPG Mixed Collocation Method for Solving Inverse Problems of Linear Isotropic/Anisotropic Elasticity with Simply/Multiply-Connected Domains. *CMES: Computer Modeling in Engineering & Sciences,* vol. 94, pp. 1-28.

Zhong, Y.; Xiang, J. (2011): Construction of wavelet-based elements for static and stability analysis of elastic problems. *Acta Mechanica Solida Sinica,* vol. 24, pp. 355-364.

Zhu, H.; Sankar, B. V. (2004): A combined Fourier series–Galerkin method for the analysis of functionally graded beams. *Journal of Applied Mechanics,* vol. 71,

pp. 421-424.

Appendix

The integration matrixes mentioned in this paper have the details as follows

$$\mathbf{\Gamma}_1^{0,0} = \mathbf{T}^T \left(l_{ex} \int_0^1 \mathbf{\Phi}^T \mathbf{\Phi} \mathrm{d}\xi \right) \mathbf{T} \tag{A1}$$

$$\mathbf{\Gamma}_1^{0,1} = \mathbf{T}^T \left(\int_0^1 \mathbf{\Phi}^T \frac{\mathrm{d}\mathbf{\Phi}}{\mathrm{d}\xi} \mathrm{d}\xi \right) \mathbf{T} \tag{A2}$$

$$\mathbf{\Gamma}_1^{1,0} = \mathbf{T}^T \left(\int_0^1 \frac{\mathrm{d}\mathbf{\Phi}^T}{\mathrm{d}\xi} \mathbf{\Phi} \mathrm{d}\xi \right) \mathbf{T} \tag{A3}$$

$$\mathbf{\Gamma}_1^{1,1} = \mathbf{T}^T \left(\frac{1}{l_{ex}} \int_0^1 \frac{\mathrm{d}\mathbf{\Phi}^T}{\mathrm{d}\xi} \frac{\mathrm{d}\mathbf{\Phi}}{\mathrm{d}\xi} \mathrm{d}\xi \right) \mathbf{T} \tag{A4}$$